

2



NRL Memorandum Report 6468
(Revised NRL Memorandum Report 5862)

AD-A209 722

Monitoring Sources of Nuclear Radiation in Space 1980-1984 Observations

G.H. SHARE AND J.D. KURFESS

*Gamma and Cosmic Ray Astrophysics Branch
Space Science Division*

D.C. MESSINA

*Sachs/Freeman Assoc., Inc.
Landover, MD 20785*

DTIC
SELECTE
JUL 08 1989
S
D

May 31, 1989

REPORT DOCUMENTATION PAGE				Form Approved OMB No 0704-0188	
1a REPORT SECURITY CLASSIFICATION UNCLASSIFIED		1b RESTRICTIVE MARKINGS			
2a SECURITY CLASSIFICATION AUTHORITY		3 DISTRIBUTION / AVAILABILITY OF REPORT Approved for public release; distribution unlimited.			
2b DECLASSIFICATION / DOWNGRADING SCHEDULE		5 MONITORING ORGANIZATION REPORT NUMBER(S)			
4 PERFORMING ORGANIZATION REPORT NUMBER(S) NRL Memorandum Report 6468 (Revised NRL Memorandum Report 5862)		5 MONITORING ORGANIZATION REPORT NUMBER(S)			
6a NAME OF PERFORMING ORGANIZATION Naval Research Laboratory		6b OFFICE SYMBOL (If applicable) Code 4150	7a NAME OF MONITORING ORGANIZATION		
6c. ADDRESS (City, State, and ZIP Code) Washington, DC 20375-5000		7b ADDRESS (City, State, and ZIP Code)			
8a NAME OF FUNDING / SPONSORING ORGANIZATION Office of Naval Research	8b OFFICE SYMBOL (If applicable)	9 PROCUREMENT INSTRUMENT IDENTIFICATION NUMBER			
8c. ADDRESS (City, State, and ZIP Code) Arlington, VA 22217		10 SOURCE OF FUNDING NUMBERS			
	PROGRAM ELEMENT NO	PROJECT NO	TASK NO	WORK UNIT ACCESSION NO	
11 TITLE (Include Security Classification) Monitoring Sources of Nuclear Radiation in Space: 1980-1984 Observations					
12 PERSONAL AUTHOR(S) Share, G.H., Kurfess, J.D. and Messina,* D.C.					
13a TYPE OF REPORT Interim	13b TIME COVERED FROM 4/80 TO 1/85	14. DATE OF REPORT (Year, Month, Day) 1989 May 31		15 PAGE COUNT 32	
16 SUPPLEMENTARY NOTATION *Sachs/Freeman Associates, Inc., Landover, MD 20785					
17 COSATI CODES			18 SUBJECT TERMS (Continue on reverse if necessary and identify by block number)		
FIELD	GROUP	SUB-GROUP	RORSAT Gamma-radiation Space nuclear reactors Trapped-radiation		
19 ABSTRACT (Continue on reverse if necessary and identify by block number) <p>The gamma-ray spectrometer (GRS) on NASA's Solar Maximum Mission satellite (SMM) made its initial detection of nuclear radiation from a reactor-powered spacecraft in 1980 when COSMOS 1176 was launched by the Soviet Union. This class of spacecraft has the acronym RORSAT for Radar Ocean Reconnaissance SATellite. SMM observed radiation from each of the subsequently launched RORSATS: COSMOS 1249 in 1981; 1365, 1372, and 1402 in 1982; 1579 and 1607 in 1984; 1670 and 1677 in 1985. Direct observations of gamma radiation were made within about 500 km when the RORSATS were not occulted by a significant amount of material in SMM. Indirect observations were also made up to distances in excess of a few thousand kilometers. These observations were made when positrons</p> <p style="text-align: right;">(Continues)</p>					
20 DISTRIBUTION / AVAILABILITY OF ABSTRACT <input checked="" type="checkbox"/> UNCLASSIFIED/UNLIMITED <input type="checkbox"/> SAME AS RPT <input type="checkbox"/> DTIC USERS			21 ABSTRACT SECURITY CLASSIFICATION UNCLASSIFIED		
22a NAME OF RESPONSIBLE INDIVIDUAL G.H. Share		22b TELEPHONE (Include Area Code) (202) 767-3165		22c OFFICE SYMBOL Code 4150	

19. ABSTRACTS (Continued)

and electrons produced in the outer layers of the reactor-powered spacecraft reached SMM after being stored in the geomagnetic field.

In this report we provide details of SMM's observations of the seven RORSATS launched from 1980 through 1984. We obtain estimates of the relative power of the reactors from integral gamma-ray intensities measured at distances <400 km. The average intensities from the seven satellites, after correcting for distance of separation, are consistent with each other to within 30%. In contrast, the rate of distant detections of positrons increased with time over the four-year period. The rate of detections was about 0.2/day in 1980 and 0.7/day in 1984. We suggest that this increasing rate is due to the decreasing atmospheric density above a few hundred km in the transition from maximum to minimum solar activity. The positron storage time in the geomagnetic field is expected to increase with decreasing density.

A composite gamma-ray spectrum created from a summation of close-approach sightings of the seven RORSATS will be presented. It is not possible to obtain a unique interpretation of this spectrum. One relatively simple model of the gamma-ray spectrum emitted from the RORSATS which fits the data reasonably well includes the following components: a fission continuum from ^{235}U and neutron capture lines from molybdenum embedded within tens of g/cm^2 of material; two unresolved lines near 500 keV attributed to a line at 511 keV from positron-annihilation and to a line near 477 keV from boron. Other neutron capture lines may contribute to the observed spectrum. An estimate is made of the capability of a high-resolution spectrometer to identify the individual spectral features.

CONTENTS

I.	INTRODUCTION	1
II.	DISTANT DETECTIONS OF RORSATS	2
III.	RELATIVE GAMMA-RAY INTENSITIES FROM RORSATS	4
IV.	GAMMA-RAY EMISSION SPECTRUM OF RORSATS	5
	A. GAMMA-RAY VS NEUTRON ORIGIN	5
	B. INTERPRETATION OF THE SPECTRUM	6
	C. HALF MEV FEATURE	7
	D. HIGH-ENERGY EMISSION	8
V.	POTENTIAL FOR HIGH RESOLUTION SPECTROSCOPY	10
VI.	SUMMARY	12
VII.	ACKNOWLEDGMENTS	13
VIII.	REFERENCES	13



Accession For	
DTIC CRA&I	<input checked="" type="checkbox"/>
DTIC TAB	<input type="checkbox"/>
Unannounced	<input type="checkbox"/>
Justification	
By _____	
Date _____	
A-1	

MONITORING SOURCES OF NUCLEAR RADIATION IN SPACE

1980-1984 OBSERVATIONS

I. INTRODUCTION

The gamma-ray spectrometer on NASA's Solar Maximum Mission satellite (SMM) first detected radiation from a nuclear reactor in space in 1980, following the launch of COSMOS 1176. COSMOS 1176 was one of a series of Soviet satellites with the acronym RORSAT, which stands for Radar Ocean Reconnaissance SATellite. Details of the history of these measurements can be found in an earlier report (Share, Kurfess, Marlow, et al. 1989). Direct observations of gamma radiation were made within about 500 km when the view of the RORSAT was not blocked by a significant amount of material in SMM. Indirect observations were also made at distances up to in excess of a few thousand kilometers when positrons and electrons produced in the outer layers of the RORSAT were detected by the SMM spectrometer after being stored in the geomagnetic field. The positrons were unambiguously identified by the 0.511 MeV gamma-ray line produced when they annihilated in local material near the spectrometer.

Spectral measurements during four close encounters with COSMOS 1176 were detailed. The spectrum of radiation was hard and extended up to about 7 MeV, above which energy the intensity fell off rapidly. This high-energy feature was attributed to neutron-capture gamma rays from either beryllium or molybdenum in the reactor or from the interactions of neutrons from the reactor interacting in SMM's NaI detector. We were not able to unambiguously identify the source of the radiation. A feature near 0.5 MeV was also apparent in the spectra which was broader than the instrument's response to a narrow line. We attributed this feature to a blend of lines including the positron-electron annihilation line at 0.511 MeV.

Twenty-six annihilation events were detected by SMM that were attributable to positrons emitted by COSMOS 1176. Some of these detections were made when SMM and COSMOS were separated by more than 5000 km. By using the locations of the spacecraft and an algorithm for tracing particles in the geomagnetic field, we showed that most of the events could be explained by positrons emitted by COSMOS 1176 which temporarily filled a magnetic flux tube traversed by SMM. In most cases there was clear evidence for the expected westward drift of the positrons prior to detection by the spectrometer. Several charged-particle events were also detected by plastic scintillation detectors in both the GRS and the Hard X-ray Burst Spectrometer experiment on SMM. For these events there was clear evidence for an eastward drift of the electrons in the geomagnetic field. Hones and Higbie (1989) have performed detailed calculations which confirm this magnetic storage origin for the annihilation and charged-particle events observed by SMM.

Manuscript approved April 17, 1989.

The gamma-ray spectrometer has been in almost continuous operation since its launch in 1980; its performance has been excellent and stable. With the exception of a six-month period from October 1983 to April 1984, when SMM's tape recorders were turned off, it has proved to be a monitor of Soviet nuclear reactors in space. In April 1984 SMM's attitude control system was repaired by the Shuttle astronauts. Although the satellite was not boosted up to 550 km as planned, it is expected to remain in a stable orbit until at least 1991. NASA has been considering the possibility of retrieving SMM in 1990 in order to refurbish the Multi-Mission portion of the spacecraft for use by other experimental payloads in the 1990's.

The SMM spectrometer has observed radiation from each of the subsequently launched RORSATS: COSMOS 1249 in 1981; 1365, 1372, and 1402 in 1982; 1579 and 1607 in 1984; 1670 and 1677 in 1985. This report summarizes measurements of nuclear radiation emitted from the seven RORSATS launched by the Soviet Union from 1980 to 1984. The RORSATS COSMOS 1579 and 1607 were launched on June 29 and October 31, 1984, respectively, and were the first to be put into orbit following the well publicized re-entry of COSMOS 1402 in February 1983. This paper supercedes an earlier preliminary report (Share, Kurfess, and Messina 1989) which primarily discussed observations of COSMOS 1579. COSMOS 1670 and 1677 were launched in the summer of 1985; a report describing the SMM observations of these satellites is in preparation.

In the next section we discuss the detections of positrons emitted by the RORSATS and stored in the geomagnetic field. The number of such detections has increased with time. We suggest that this increase is due to the effects of solar radiation on the upper atmosphere. Section III treats the integral gamma-ray intensities measured at distances <400 km for the seven RORSATS launched from 1980 to 1984. We show that these intensities, when normalized to the same distance, are consistent with each other and suggest that the basic operational characteristics of the reactors are the same. Section IV presents a composite spectrum of the nuclear radiation derived from all measurements of seven RORSATS made at distances <400 km and well within the broad aperture of the SMM spectrometer. We utilize the instrument response function to obtain an estimate of the spectrum of gamma radiation emitted by the satellites. This model spectrum is then used in Section V to provide an estimate of what additional information can be obtained using high-resolution germanium spectrometers.

II. DISTANT DETECTIONS OF RORSATS

One of the early puzzling aspects of SMM's detection of radiation from the RORSATS was the mechanism that produced bursts of annihilation line radiation (0.511 MeV) and charged particles. This was explained by the storage of positrons and electrons emitted from the RORSATS in the geomagnetic field (Share, Kurfess, Marlow, et al. 1989). The rate of these detections provides a means of monitoring the radiation from RORSATS on time scales of a few days.

We have performed an automated search for bursts of annihilation line radiation in SMM data from 1980 through January 1985. Any bursts identified by this computer algorithm were visually screened in order to exclude extraneous events resulting from bad telemetry, solar flares, etc. True bursts of 0.511 MeV gamma rays were found only during periods when a Soviet RORSAT was known to be in operation.

Our analysis indicates that the overall rate of these 0.511 MeV events has increased in time from 1980 to 1984. This is shown in Figure 1 where we have plotted the number of events/(day of RORSAT operation). This rate has been determined for each of the years. A single RORSAT was in operation during each of the first two years 1980 and 1981; however there were three RORSATS in operation in 1982 and two in operation in 1984. For the latter two years, we did not try to identify the bursts with a specific satellite but, instead, determined an average rate for the year. There is a striking increase in the rate of annihilation line events from 1980 to 1984. It is not likely to be due to any progressive changes in the power of the reactors as we will show in the next section; therefore it is likely that the increase is due to either an orbital or geophysical effect.

As shown on the top scale in Figure 1, SMM dropped in altitude from 570 km in 1980 to 500 km in 1984. This reduction in altitude should have lead to a reduction, not an increase, in the number of annihilation events because the trapped positrons which can reach SMM will mirror at a lower altitude and therefore suffer greater losses in the denser atmosphere.

A likely explanation for the increasing rate of 0.511 MeV line events with time is the decreasing density of the upper atmosphere from 1980 to 1984. When SMM was launched in 1980 solar activity was at its peak. By 1984 the activity had diminished by a factor of about three, as monitored by the monthly mean sunspot number. The atmospheric density at 200 km decreases by a factor of about five from solar maximum to the solar minimum. This implies that positrons emitted from the RORSATS at 260 km are expected to encounter vastly different scattering environments in 1980 and 1984. Hones and Higbie (1989) have made a detailed calculation of the propagation and losses of positrons released into the geomagnetic field. They show that the scattering life time of the positrons is inversely proportional to the atmospheric density. From this we conclude that positrons emitted during the minimum of the solar cycle can be stored in the geomagnetic field up to about five times longer than during the maximum. This means that the probability that SMM will enter an L shell in which the positrons are resident is up to a factor of five higher during solar minimum.

We conclude that the decrease in the density of the upper atmosphere from solar maximum to solar minimum is the likely source of the increase in the rate of annihilation line events shown in Figure 1. Detailed analysis of the time structure of the annihilation events and the time delay from injection of the positrons into the geomagnetic field can confirm this model.

III. RELATIVE GAMMA-RAY INTENSITIES FROM RORSATS

The excellent gain stabilization of the SMM spectrometer allows us to determine the relative gamma-ray emissivities of the seven RORSATS in operation from 1980 through the end of 1984. We utilize the integral rate of gamma-rays in the energy range from 0.8 to 8.0 MeV during close-approach (< 400 km) sightings when the RORSATS were within about 70° of the detection axis of the instrument. We chose this energy range in order to reduce effects due to absorption of the emission in any intervening material. The rates were integrated over the 49 s period when the RORSATS were closest to SMM. The background was estimated from rates observed within a few minutes of the detection. The difference between the on-source and background rates were then normalized to detection at an average separation of 300 km, under the assumption that the emission is isotropic. We have only included sightings for which we have confidence that the background is well determined.

Our measurements of the integral 0.8 - 8.0 MeV gamma-ray intensities from all of the usable sightings of the seven RORSATS are plotted in Figure 2. The errors shown include the statistical uncertainties in the on-source and background counting rates, and the uncertainty in the mean separation of the satellites. The measured rates range from about 250 to 400 cts/16 s interval (normalized to a separation of 300 km). There is no evidence for any significant variation in intensity either from satellite to satellite or within the operational period of a given system.

The average gamma-ray intensities (300 km separation) in the 0.8 - 8.0 MeV range measured for each of the seven RORSATS is given in Table 1. The mean rate for all the satellites is 322 cts/16 s. The distribution of rates is somewhat broader than what would be expected for random sample, but we believe that there is no clear evidence for a systematic variation from satellite to satellite.

TABLE 1

Average Gamma-Ray Rates (0.8 - 8.0 MeV) From RORSATS

Satellite COSMOS #	Rate cts/16 s
1176	360 \pm 30
1249	282 \pm 37
1365	364 \pm 44
1372	309 \pm 32
1402	270 \pm 24
1579	349 \pm 22
1607	321 \pm 24

IV. GAMMA-RAY EMISSION SPECTRUM OF RORSATS

We have studied the emitted gamma-ray spectra from RORSATS observed by the SMM spectrometer from 1980 to the beginning of 1985. These spectra were obtained from the close-approach sightings used to determine the integrated 0.8 - 8.0 MeV intensities discussed in the preceding section. Visual inspection of these spectra indicates that the gross features of the gamma-ray emissions from the individual spacecraft do not differ significantly. In order to obtain information concerning the design of the reactors we have assumed that all the RORSATS have the same design, and therefore have summed all the background corrected spectra.

An integrated count-rate spectrum from close-approach sightings of the seven RORSATS is shown in Figure 3. This spectrum was accumulated in 1470 s when SMM was within about 400 km of the COSMOS satellites. For purposes of presentation, the original 476 channel spectrum has been compressed so that the plotted rates in each channel are statistically significant.

A. GAMMA-RAY VS NEUTRON ORIGIN

Before we can address the interpretation of the features of the spectrum, we must first resolve a fundamental question concerning the source. In our earlier report (Share, Kurfess, Marlow, et al. 1989), we concluded that the spectrum could have either been produced by gamma rays or neutrons emitted from the RORSATS. We list below the arguments that lead us to conclude that the dominant contribution comes from gamma radiation from the RORSATS:

1. Thermal neutrons from the reactor are ruled out because they would take a few minutes to reach SMM; this conflicts with the observed time variations.
2. The off-axis response to the radiation is consistent with a gamma-ray origin; fast neutrons would have produced significantly less off-axis attenuation than observed.
3. The observed spectrum is too hard to be consistent with what is expected from fission neutrons inelastically scattering in the NaI detector (see Bendt and Journey, 1978). Furthermore there is not enough material surrounding the detector to thermalize a large fraction of the neutrons and thereby produce a harder neutron capture spectrum.
4. The flux of MeV gamma radiation from unshielded nuclear reactors is at least comparable to (Robitaille and Hoffarth 1980) or several times the neutron flux (Goldstein 1959; Gabro and Mooney 1961 [assuming 6 inch lead shielding surrounding the ASTR was removed]).
5. The interaction cross section in the SMM NaI detectors is higher for gamma-rays than for fast neutrons.

B. INTERPRETATION OF THE SPECTRUM

The general features of the spectrum shown in Figure 3 are similar to what we described in our first report (Share, Kurfess, Marlow, et al. 1989), which detailed measurements of COSMOS 1176. The spectrum is hard with emission extending up to at about 7 MeV, above which energy the rate falls rapidly. Aside from this high-energy cutoff, the most striking feature occurs near 500 keV. These two significant spectral features provide the most unambiguous information concerning the makeup of the reactor. There is also considerable information both in the shape of the continuum and in apparent weaker features, but the interpretation derived is not unique. This is true because these shapes can arise from a combination of a variety of sources embedded in an undetermined amount of material.

The determination of the emitted gamma-ray spectrum from the RORSATS is not a unique process. We therefore start with some assumed input spectrum, which we then fold through the instrument response function, to obtain a predicted count-rate spectrum that can be compared with the data. From a compilation of published reports on COSMOS 954 a composite picture has been constructed of the design of the RORSATS (Bennett 1989). It includes a reactor constructed of 90% ^{235}U and 10% Mo fuel elements and Be neutron reflectors. A detailed estimate of the emitted gamma-ray spectrum would utilize a sophisticated transport code which takes into account the detailed geometry of the reactor and its nearby structure. This was not possible in the current study. We've therefore made some basic approximations in order to obtain some information from the count rate spectra.

We assume that the gamma-ray emitting regions of the reactor are either contained under about 50 g/cm^2 or 7 g/cm^2 of overlying material. We further assume that the material has the scattering properties of Al. Sources from within the reactor itself, such as the Mo, are assumed to lie under the thick scatterer, 50 g/cm^2 . The fission gamma-ray spectrum of ^{235}U after neutron irradiation of at least $2 \times 10^4 \text{ s}$ has been measured by Bendt and Journey (1978). This spectrum was modified by scattering in the thick scatterer and was then passed through the instrument response function. The results of this calculation are shown by the curve plotted in Figure 3 which was adjusted vertically by eye to provide a good fit to the data below a few MeV. The general shape of the fission gamma-ray spectrum fits the measured continuum below about 3 MeV, but cannot account for the emission observed at higher energies. It also does not account for the 0.5 MeV feature. We next address this 0.5 MeV feature.

C. HALF MEV FEATURE

Fits to the this feature indicate that it can be accounted for by either a broadened line with an energy of about 490 keV or a blend of two lines. As we know of no plausible broadened line feature near 490 keV, we assume that the feature is caused by two unresolved lines. As evident from SMM's distant detection of positrons from RORSATS, a strong line at 0.511 MeV due to electron-positron annihilation radiation from the reactor is expected. When we fit the data with a narrow line fixed at 511 keV and ask what the best fit energy is for another narrow line at lower energy, we obtain a value of 473 ± 4 keV. The measured intensity of the 473 keV line is $(8.1 \pm 1.3) \times 10^{-3}$ /cm²-s, while the intensity of the 511 keV line is $(6.7 \pm 1.3) \times 10^{-3}$ /cm²-s.

Three possible materials can account for a line near 473 keV. These are Na, Li, and B. Neutron capture on Na produces a strong line at 472.4 keV, which is produced in 60% of the radiative captures (Lone et al. 1981), and other weaker lines (e.g. 870 keV, 22%; 2.027 MeV, 17%; 3.983 MeV, 19%; 6.395 MeV, 22%) at higher energy. Liquid sodium is a possible candidate for the coolant used in the RORSATS (Bennett 1989). Neutron capture on Li produces a line at 477.6 keV which is observed in about 3% of the captures, but it also produces a strong line at 2.032 MeV that is produced in 90% of the captures. LiH is believed to be used to shield the operational satellite from neutrons emitted by the reactor (Bennett 1989). Therefore we would also expect to detect the 2.223 MeV neutron capture line from hydrogen if the 477.6 MeV Li line were present. Bennett (1989) indicates that B is present in the control mechanism for moving the Be reflectors control cylinders. The (n, α) reaction on ¹⁰B (20 % of natural boron) has a very large cross section and produces a 477.6 keV gamma-ray line from the excited state of ⁷Li. (We note that there is a strong line at 479.6 keV following the beta decay of ¹⁸⁷W produced in neutron capture on tungsten, but there is no evidence in the data for the more intense line expected at 680 keV. Therefore tungsten is not likely to be a major contributor to the feature near 0.5 MeV. We included this discussion on tungsten here because its neutron capture lines above 4 MeV may help explain some of the structure appearing in the measured spectrum. This is discussed below).

It is possible to set limits on the contribution of some of the suggested sources of the ~473 keV line by searching for evidence of other neutron capture lines in the measured count-rate spectrum at higher energy. Shown in Figure 4 by the curve is a model spectrum including a contribution from fission of ²³⁵U a narrow line at 0.511 MeV, and neutron-capture gamma rays from Na (Lone, Leavitt, and Harrison 1981), after passing through the instrument response function. The relative intensities have been adjusted to fit the data in the 500 keV domain. In this model it was assumed that both the 0.511 MeV and Na lines were generated under only 7 g/cm² of material. Under this assumption the higher-energy capture lines from Na shown by the curve appear to marginally exceed the data. In fact, the assumption that the Na lies under only 7 g/cm² is not correct. Any Na which is likely to produce a significant number of neutron captures will be embedded in the cooling tubes of the reactor. For this reason what is plotted in Figure 4 is a best case situation. If we

place the Na under 50 g/cm², then any associated emission near 0.5 MeV is very strongly attenuated relative to the higher-energy lines. These high-energy lines then dominate the spectrum when we attempt to fit the half MeV feature, and provide a totally unacceptable fit. From this we conclude that Na is not the dominant source of the ~473 keV line.

We can use the same arguments to exclude Li as a source of the ~473 keV feature. Shown in Figure 5 is a fit to the ~473 keV feature assuming that it came from neutron capture on LiH. It is clearly inconsistent with the data.

We conclude from the results plotted in Figures 4 and 5 that neutron capture lines from neither Na or LiH can explain a significant part of the ~473 keV line. It is more likely that the boron near the reactor is the source of the ~473 keV line. The solid curve drawn in Figure 6 is the expected response of the detector to a model source emitting a fission spectrum under 50 g/cm² and narrow 477 and 511 keV lines under 7 g/cm² of material. This model provides a good fit to the data below about 3 MeV. Additional sources are required at higher energy. This is addressed below.

D. HIGH-ENERGY EMISSION

We have attempted to determine the source of the emission above 3 MeV observed from the RORSATS. As seen in Figures 3-6, the most striking feature is the fairly sharp cutoff above about 7 MeV. There also appears to be some broad features in the spectrum at lower energies. This high-energy emission could come from radiative thermal neutron capture or fast neutron interactions on materials within and near the reactor, or from radioactive products of these reactions. Based on available information (Bennett 1989), the most likely materials in and around the reactor are molybdenum, beryllium, sodium/potassium, iron, boron, and lithium hydride.

There are not many radioactive isotopes of these materials, or others for that matter, above about 5 MeV (Bowman and Macmurdo 1974). Most of the isotopes in this energy range are fission products and therefore should be contained within the fission spectrum we've utilized from Bendt and Journey (1978). The only other line from a radioactive decay in materials near the reactor is from ¹¹Be at 6.79 MeV, but in this case we should see a strong line at 2.12 MeV as well. It is therefore not likely that the emission above 4 MeV is from radioactive isotopes.

Fast neutrons which interact in the molybdenum within the reactor core produce a structured continuum which extends up to at least 7 MeV (Morgan and Newman 1975). The shape of the emitted spectrum is dependent on the spectrum of fast neutrons. We have used a weighted sum of two of the published spectra for incident neutrons between 0.6 and 1.0 MeV and 3.0 to 3.5 MeV to approximate what might be expected from a reactor. The resultant spectrum after passing through 50 g/cm² of material does not appear to be hard enough to account for the observed emission from the RORSATS. This can be seen in Figure 7 which shows a solid line representing a model containing both fission and fast neutron

gamma-rays from the reactor core and the blended line features near 0.5 MeV. The fit below 4 MeV is acceptable but the model does not describe the data at higher energies.

The most likely sources of the high-energy emission from the RORSATS are neutron capture gamma-rays. Both molybdenum and beryllium produce neutron capture gamma-rays near 7 MeV (Lone, Leavitt and Harrison 1981). Molybdenum emits a gamma ray at 6.919 MeV in about 3% of radiative neutron captures and beryllium emits a 6.809 MeV gamma ray in about 64% of these captures. Beryllium emits 8 other lines at lower energy, while molybdenum emits over 150 additional lines. We have constructed two source models which include the two narrow line features near 0.5 MeV under about 7 g/cm², the ²³⁵U fission spectrum under about 50 g/cm², and separately treat the capture gamma-ray lines from Mo and Be under about 50 g/cm². The source spectra were passed through the SMM instrument response function and compared with the observed counting rate data. The results of this analysis are shown in Figures 8 and 9 for molybdenum and beryllium, respectively.

The line drawn in Figure 8 represents what one would expect for a source dominated by neutron captures in molybdenum, fission, and the 0.5 MeV lines. The relative contributions have been adjusted manually to provide a fit to the data. The general shape of this model fits the data fairly well; however the structure in the data near 4 and 6 MeV, if real, is not fit well by the model. There is also some excess emission observed above 7 MeV. This could come from neutron capture gamma rays from the stainless steel. We show the results of including this contribution below.

The model consisting of neutron capture on Be fits the data considerably worse, as can be seen in Figure 9. It does not contain enough of a contribution to the observed spectrum between 4 and 6.5 MeV. Inspection of Figures 4 and 5 reveals that Na and LiH by themselves do not provide neutron capture gamma-ray spectra that fit the observed data. Potassium may be contained in the coolant for the reactor. Its neutron capture cross section is also a factor of five higher than sodium; therefore if NaK is the coolant, neutron capture gamma-rays from K could be an important component. A model spectrum having a strong K source, embedded under 50 g/cm², doesn't fit the data well above 4 MeV. As boron is the likely source of the 477 keV feature observed at lower energy, we investigated whether it could produce the high-energy features observed in the spectrum. The result of this study is shown in Figure 10. Boron provides a good fit to the data between 6.5 and 7 MeV, but cannot explain the 4 to 6.5 MeV region. A strong capture line at 4.443 MeV is not evident in the data.

Of the materials likely to be present within and near the reactor, molybdenum provides the best fit to the observed high-energy spectrum (Figure 7). It provides a good fit to the peak near 7 MeV and some of the structure observed at lower energies. However, as we mentioned above, it does not appear to fit the weak features observed between 4 and 6 MeV. An additional weak source above 7 MeV is also required. Stainless steel is known to have been present near the reactor and produces

relatively strong capture gamma-rays at 7.6 MeV. We therefore included iron in our model. The results are shown in Figure 11.

It is possible that a composite source including contributions from materials in addition to molybdenum may be required to fit the data. Determination of a unique model will be difficult because of the limited energy resolution of the detector and the uncertain amount of scattering material. The product of modelling such a composite spectrum is shown in Figure 12. This model includes contributions from the blended source at 0.5 MeV (see Section C above), the fission spectrum, and capture gamma-ray lines from Mo, Na, K, Be, and Fe. This model does not appear to fit the data any better than a model with capture gamma-rays from only Mo. But it is important to keep in mind that we have made no attempt at obtaining the best fit with these materials. An iterative routine using likely source materials might provide a better fit to the data.

We've noted previously that the region between 4 and 6.5 MeV is not well fit by our model, which incorporates likely materials near the reactor. We therefore searched the capture gamma-ray line tables (Lone, Leavitt and Harrison 1981) for a material that could give the desired spectral shape in that region. Tungsten shows some of these desired spectral characteristics. Shown in Figure 13 by the solid line is a model which includes the blended 0.5 MeV feature, fission, and capture gamma rays from molybdenum, beryllium, tungsten, and iron. With the exception of an unaccounted enhancement near 6 MeV, this model fits the data reasonably well. Bennett (1989) points out that tungsten may be used for shielding.

V. POTENTIAL FOR HIGH RESOLUTION SPECTROSCOPY

It is clear from the SMM results that many blended lines could be contributing to the detected spectrum. It is of interest to consider what a high resolution spectrometer would detect if it had sufficient sensitivity and exposure to the radiation from a RORSAT. Plotted in Figure 14 is the gamma-ray spectrum incident on SMM that produced the count-rate spectrum in Figure 11. This model spectrum includes contributions from ^{235}U fission and capture gamma-rays from molybdenum embedded within 50 g/cm² of material, and from 0.511 MeV (annihilation radiation), 0.477 MeV (n, α reaction on boron), and iron capture gamma-rays within 7 g/cm² of material. The lines in the model had an intrinsic width of ~ 7 keV (FWHM); however the data have been plotted using the 476 energy channels of the SMM spectrometer. These channels have widths ranging from 7 keV at 300 keV to 30 keV near 9 MeV. For this reason the plots do not represent the full capability of a germanium system, but do indicate the general features of the spectrum.

A high-resolution spectrometer can, in principle, provide important diagnostic information on the RORSATS if the model we've outlined is correct. For example, the 0.511 and 0.477 MeV lines will be resolved and identified. The source of the feature near 800 keV could also be identified. This type of instrument should also be able to resolve and identify lines above about 6 MeV. Between 1 MeV and 6 MeV there are many weak lines present, even though only two sources, molybdenum and iron, have

been included in the model (N.B. some of the line blending appearing in the figure is due to the resolution of the plots).

Our primary concern about the ability of any high-resolution system to provide new information on the design of reactor systems in space is whether it will have sufficient sensitivity and exposure time to detect enough photons from the source. In order to help in this assessment, we list in Table 2 some of the specific lines shown Figure 14. The intensities of the lines are given in $\gamma/\text{cm}^2 \text{ s}$, assuming a separation of about 300 km. We also estimate the number of photons in these lines that would be detected during a single pass of a RORSAT near a germanium spectrometer similar to the one flown on NASA's HEAO-3 satellite (Mahoney et al. 1980). It appears that an instrument of this modest size should be able to resolve and identify the blended 0.477 MeV and 0.511 MeV features even in only a single one minute observation. It may also detect and identify the 778.3 keV neutron capture line from molybdenum. A much larger instrument, longer exposure time, or closer distance of detection will be required for any of the potentially observable higher-energy lines to be detected.

TABLE 2

DETECTABILITY OF RORSATS USING GERMANIUM SPECTROMETERS

ENERGY MeV	SOURCE	INTENSITY @ 300 km $10^{-3} \quad /\text{cm}^2 \text{ s}$	ESTIMATED CTS HEAO-3 1 minute
0.477	$^{10}\text{B}(n,\alpha)\gamma\text{Li}$	8.1	12
0.511	$e^+ e^-$	6.7	10
0.778	Mo (n, γ)	4.5	5
0.848	Mo (n, γ)	2.3	2
1.091	Mo (n, γ)	0.8	0.6
1.201	Mo (n, γ)	1.0	0.6
5.712	Mo (n, γ)	2.5	0.4
6.364	Mo (n, γ)	1.4	0.2
6.625	Mo (n, γ)	1.1	0.1
6.919	Mo (n, γ)	5.3	0.5
7.631	Fe (n, γ)	0.7	0.04
7.645	Fe (n, γ)	0.7	0.04

VI. SUMMARY

This report summarizes observations by the SMM gamma-ray spectrometer of nuclear radiation emitted by the seven RORSATS launched from 1980 to 1984. These RORSATS include COSMOS 1176, 1249, 1365, 1372, 1402, 1579 and 1607. Positrons and electrons emitted from these satellites and stored in the geomagnetic field were detected at distances up to in excess of a few thousand kilometers. Measurements were also made of the emitted gamma-ray spectrum at distances within 400 km. The primary results of this study are:

1. The rate of 0.511 MeV positron-annihilation events increased from 0.2/day in 1980 to 0.7/day in 1984. This dramatic change is attributed to increased storage time of particles in the geomagnetic field due to a decrease in the density of the upper atmosphere with the transition from solar maximum to solar minimum activity.

2. Measurements of the 0.8 - 8.0 MeV gamma-radiation indicate that the thermal power produced by the seven RORSATS is the same to within 30%.

3. The observed gamma-ray spectra of the reactors appear to be similar to one another. An integrated spectrum from the seven reactors, accumulated over 1470 s, has been constructed. This spectrum exhibits a blended line feature near 0.5 MeV, a hard continuum with evidence for some structure, and a sharp cutoff above 7 MeV.

a) We conclude that the 0.5 MeV feature is likely to be due to a blending of the 0.511 MeV positron annihilation line and the 0.477 MeV line produced in (n, α) reactions on boron.

b) Various source models have been tested against the SMM data using a relatively simple algorithm. The results are not unique. A fair fit to the data is obtained with a source embedded under tens of g/cm^2 and consisting simply of fission from ^{235}U and neutron capture gamma-ray lines from molybdenum, in addition to the blended 0.5 MeV feature. The presence of other neutron capture gamma-lines from materials such as iron, beryllium, sodium, potassium, lithium, hydrogen, and tungsten has also been investigated.

4. We estimate that a one minute exposure with a germanium spectrometer similar to one flown on NASA's HEAO-3 satellite should resolve the blended 0.5 MeV feature and identify the individual lines. Identification of most of the higher features in the spectrum will require a factor of 10 to 100 increase in the effective exposure and/or sensitivity.

VII. ACKNOWLEDGMENTS

We wish to especially acknowledge our colleagues Prof. E.L. Chupp and Dr. D.J. Forrest of the University of New Hampshire. It was under their direction that this successful experiment was built. Their assistance in the understanding of the instrument's performance has been essential. Dr. J. Letaw provided assistance in developing the algorithms for forming composite model spectra. Detailed ephemeris information has been provided by R. Cote and R. Berry of NAVSPASUR. Support for the scientific analysis of the SMM data at NRL is provided by NASA contract S14513D.

VIII. REFERENCES

- Bendt, P.J. and Journey E.T. 1978, LA-7451-MS Informal Report.
- Bennett, G.L. 1989, "A Look at the Soviet Space Nuclear Power Program", Informal NASA Report (Condensed version will appear in Proceedings of the 24th Intersociety Energy Conversion Engineering Conference, Washington D.C., August 6-11, 1989).
- Bowman, W.W. and MacMurdo, K.W. 1974, Atomic and Nuclear Data Tables 13, 89-292.
- Gabro, A.N. and Mooney, L.G. 1961, Convair Corp. Document NARF-60-21T
- Goldstein, H. 1959, "Fundamental Aspects of Reactor Shielding", Addison-Wesley Publ. Co., Reading, Mass., p.113-115.
- Hones, E.W. and Higbie, P.R. 1989, Science 244, 448-451.
- Lone, M.A., Leavitt, R.A., and Harrison, D.A. 1981, Atomic Data and Nuclear Data Tables 26, 511 - 559.
- Mahoney, W.A., Ling, J.C., Jacobson, A.S., and Tapphorn, R.M. 1980, Nuclear Instr. and Meth. 178, 363-381.
- Morgan, G.L. and Newman, E. 1975, Oak Ridge National Lab. Report TM-5097.
- Robitaille, H.A., and Hoffarth, B.E. 1980, Defense Research Establishment Ottawa, Report DREO 835.
- Share, G.H., Kurfess, J.D., Marlow, K.W., Eisele, J.A., Chupp, E.L., and Strong, I.B. 1989, NRL Memorandum Report 6466.
- Share, G.H., Kurfess, J.D., Messina, D.C. 1989, NRL Memorandum Report 6467.

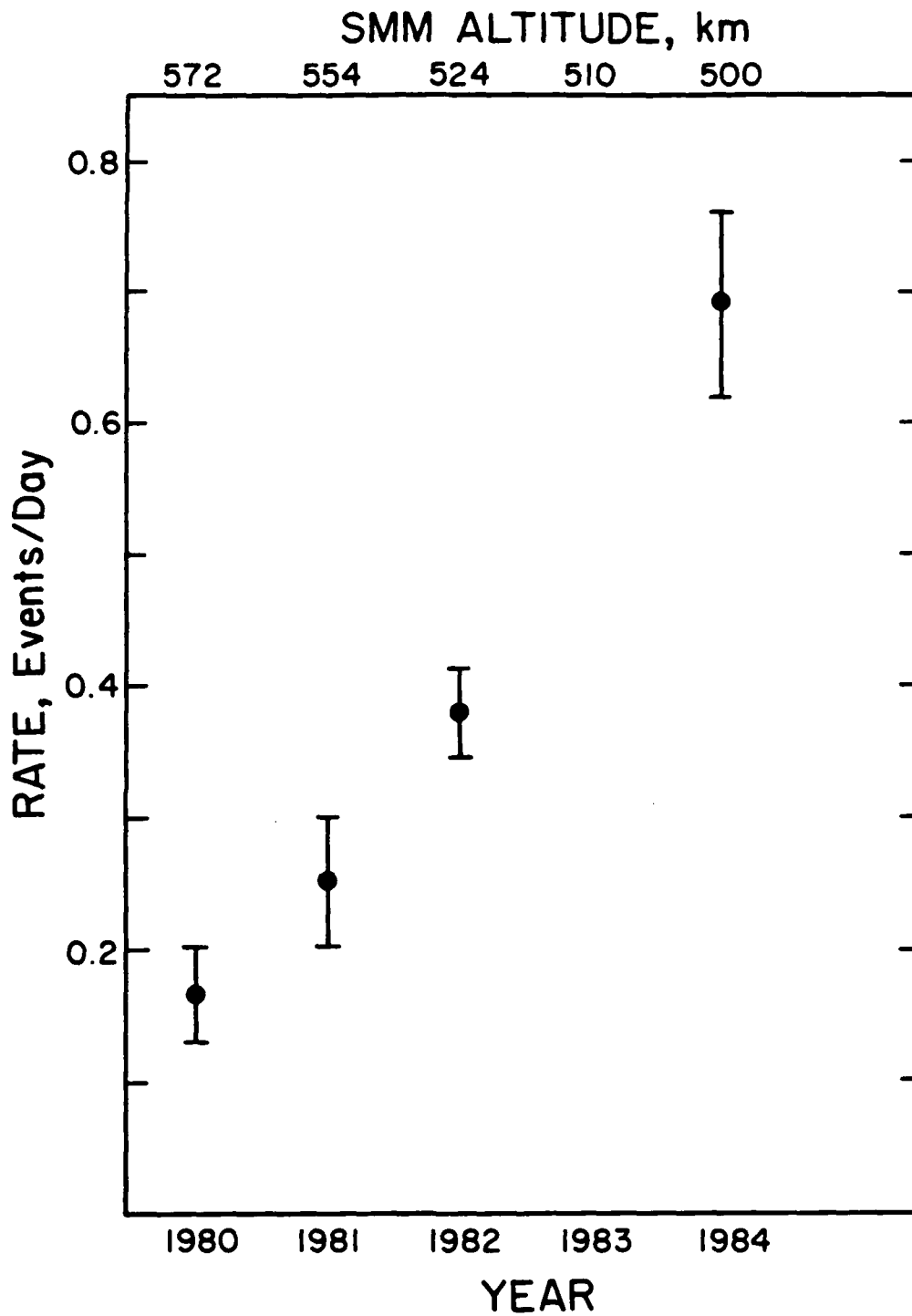


Fig. 1 - Rate of detections of bursts of annihilation radiation found in a computer search of the SMM data. Rates plotted are number of annihilation events divided by days of RORSAT operation in a given year.

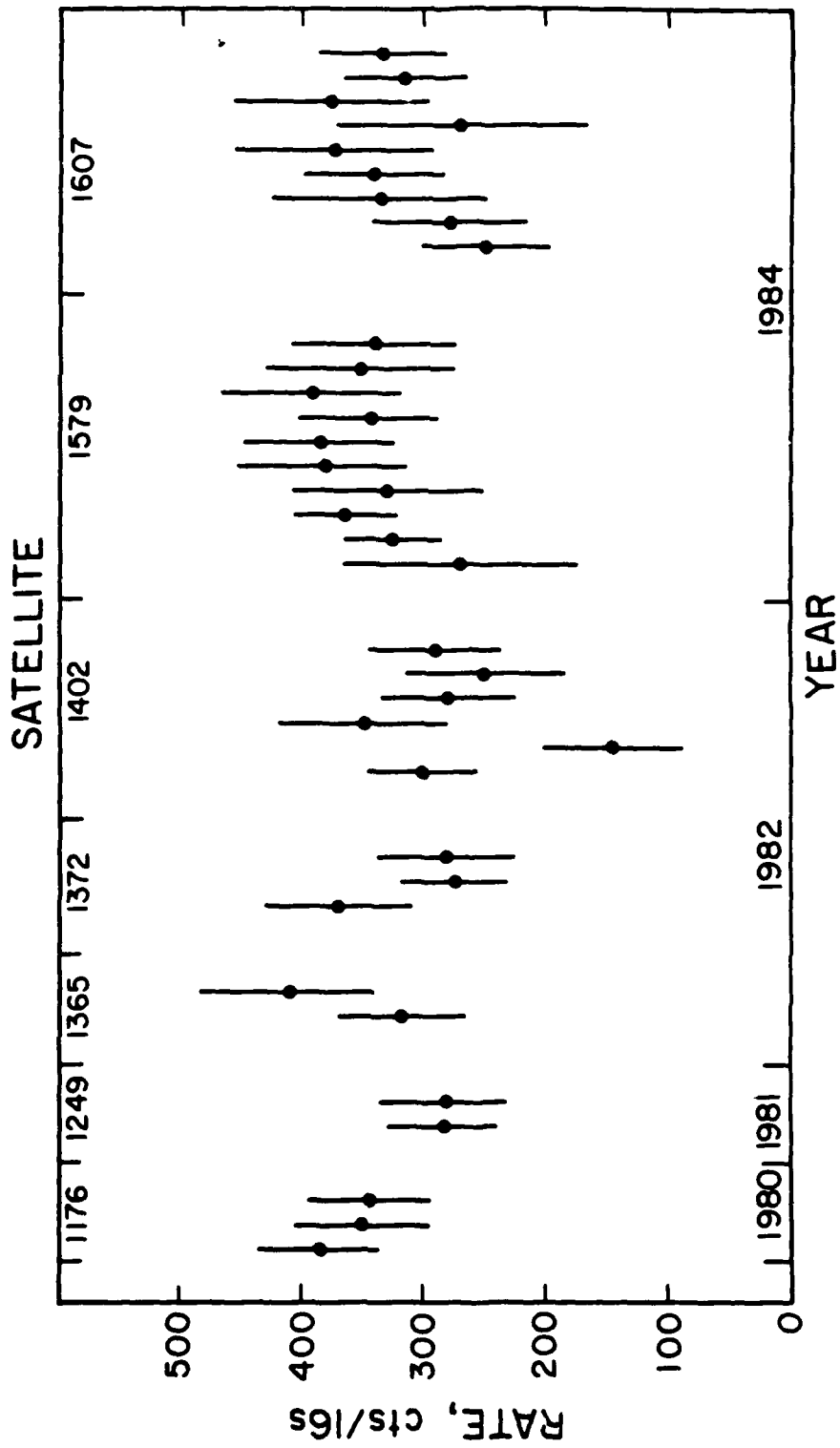


Fig. 2 — Observed 0.8 to 8.0 MeV counting rates in the SMM spectrometer, normalized to 300 km, during close-approach sightings of the seven RORSAT. Time scale within a given year is arbitrary. Identification of the RORSATS is given in the top abscissa.

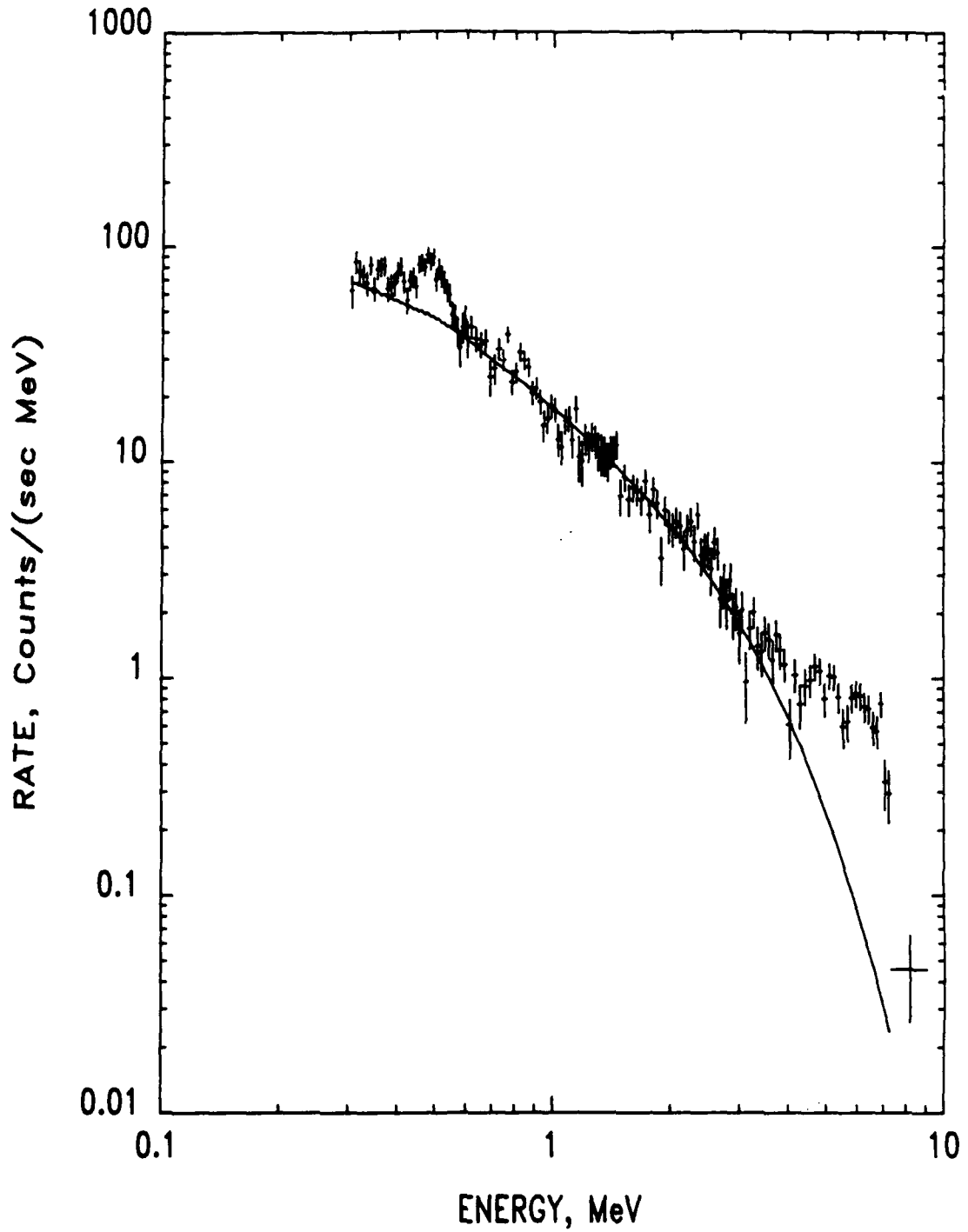


Fig. 3 - Integrated count-rate spectrum for close-approach sightings of the seven ROR-SATS in operation from 1980 to 1984. Total accumulation time is 1470 s. Curve shows ^{235}U fission spectrum after passing through 50 g/cm^2 and being modified by the instrument response function.

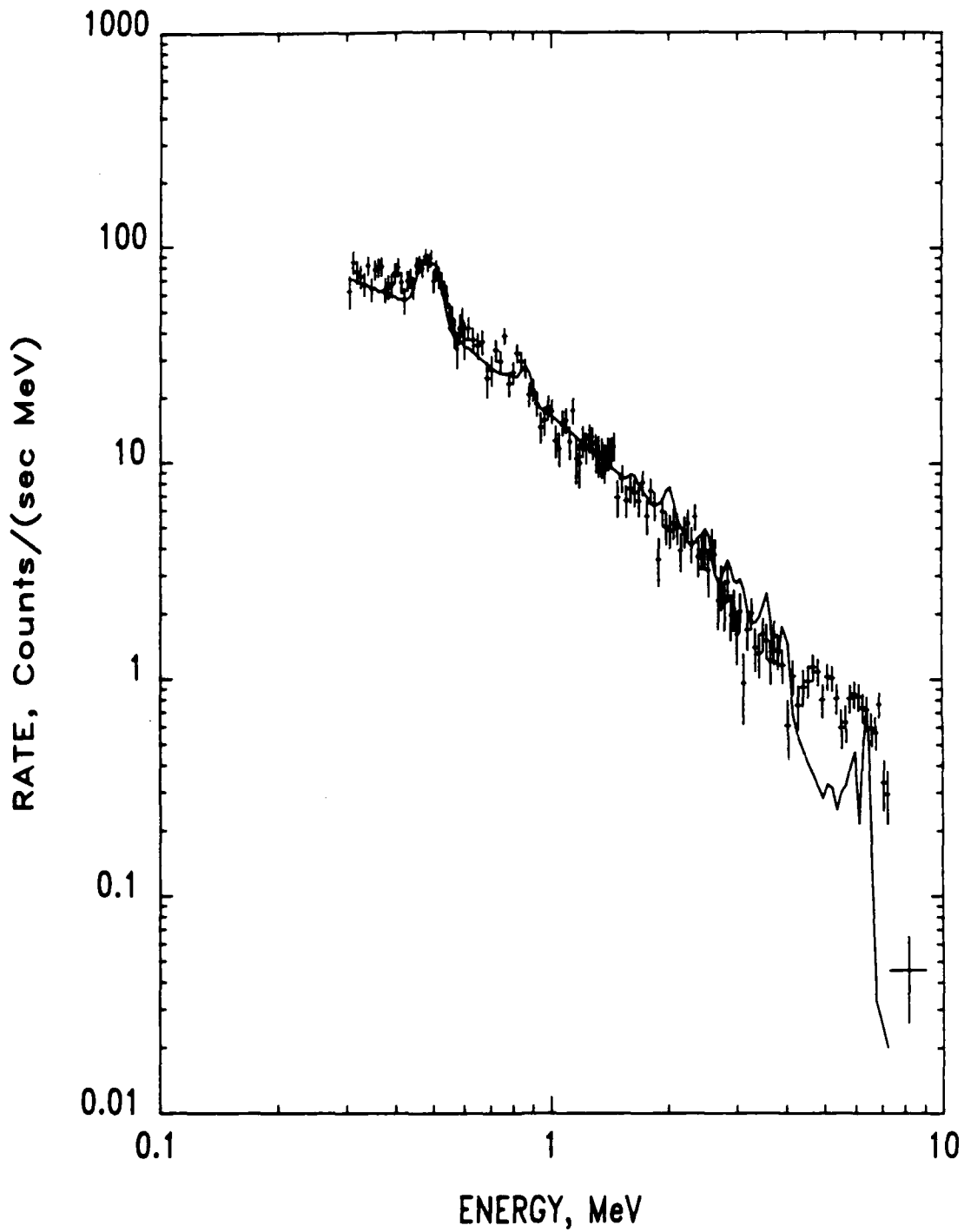


Fig. 4 — Integrated count-rate spectrum for close-approach sightings of the seven ROR-SATS in operation from 1980 to 1984. Total accumulation time is 1470 s. Curve shows composite of ^{235}U fission spectrum (under 50 g/cm^2) and Na neutron capture spectrum (under 7 g/cm^2) after being modified by the instrument response function.

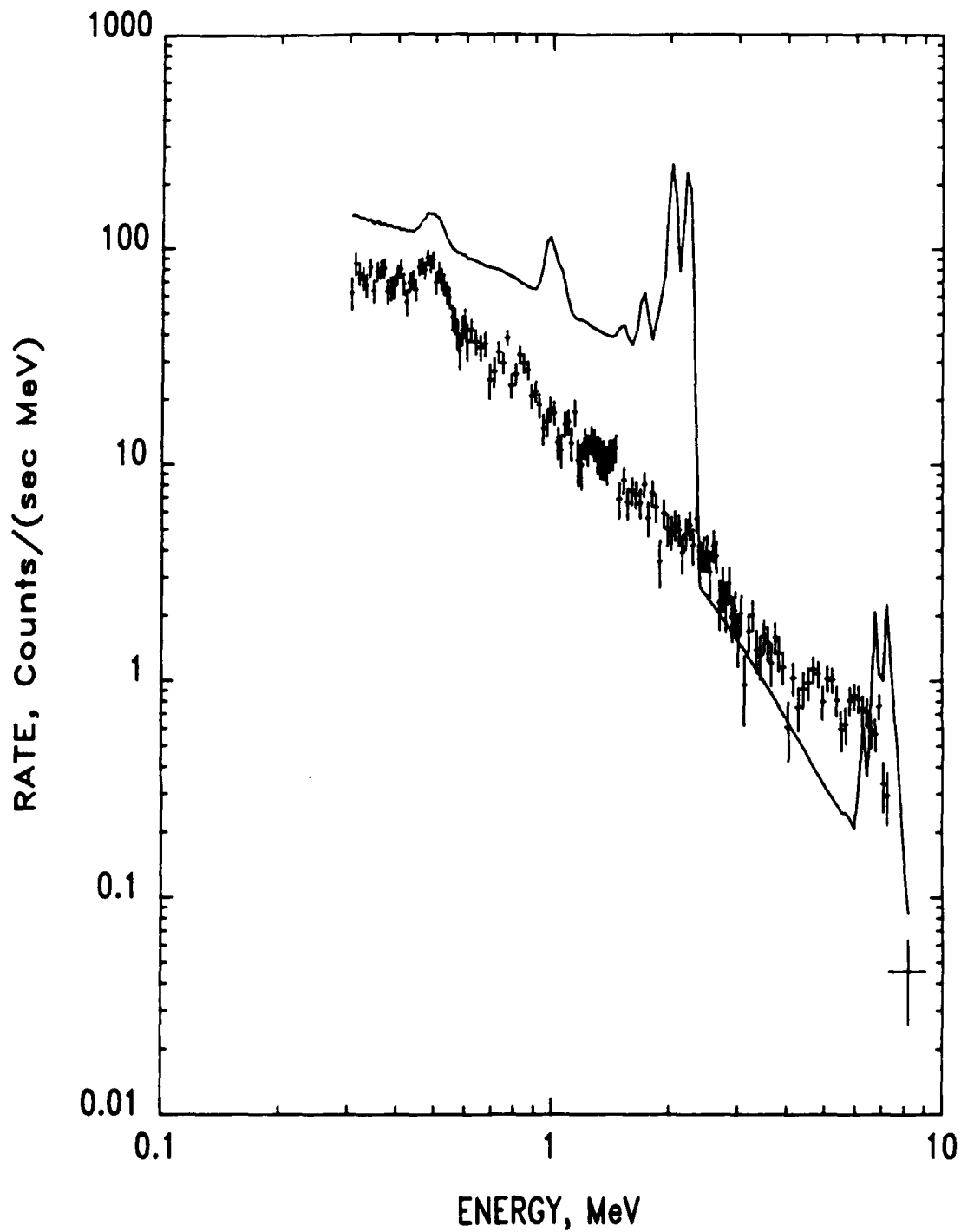


Fig. 5 - Integrated count-rate spectrum for close-approach sightings of the seven ROR-SATS in operation from 1980 to 1984. Total accumulation time is 1470 s. Curve shows composite of ^{235}U fission spectrum (under 50 g/cm^2) and LiH neutron capture spectrum (under 7 g/cm^2) after being modified by the instrument response function.

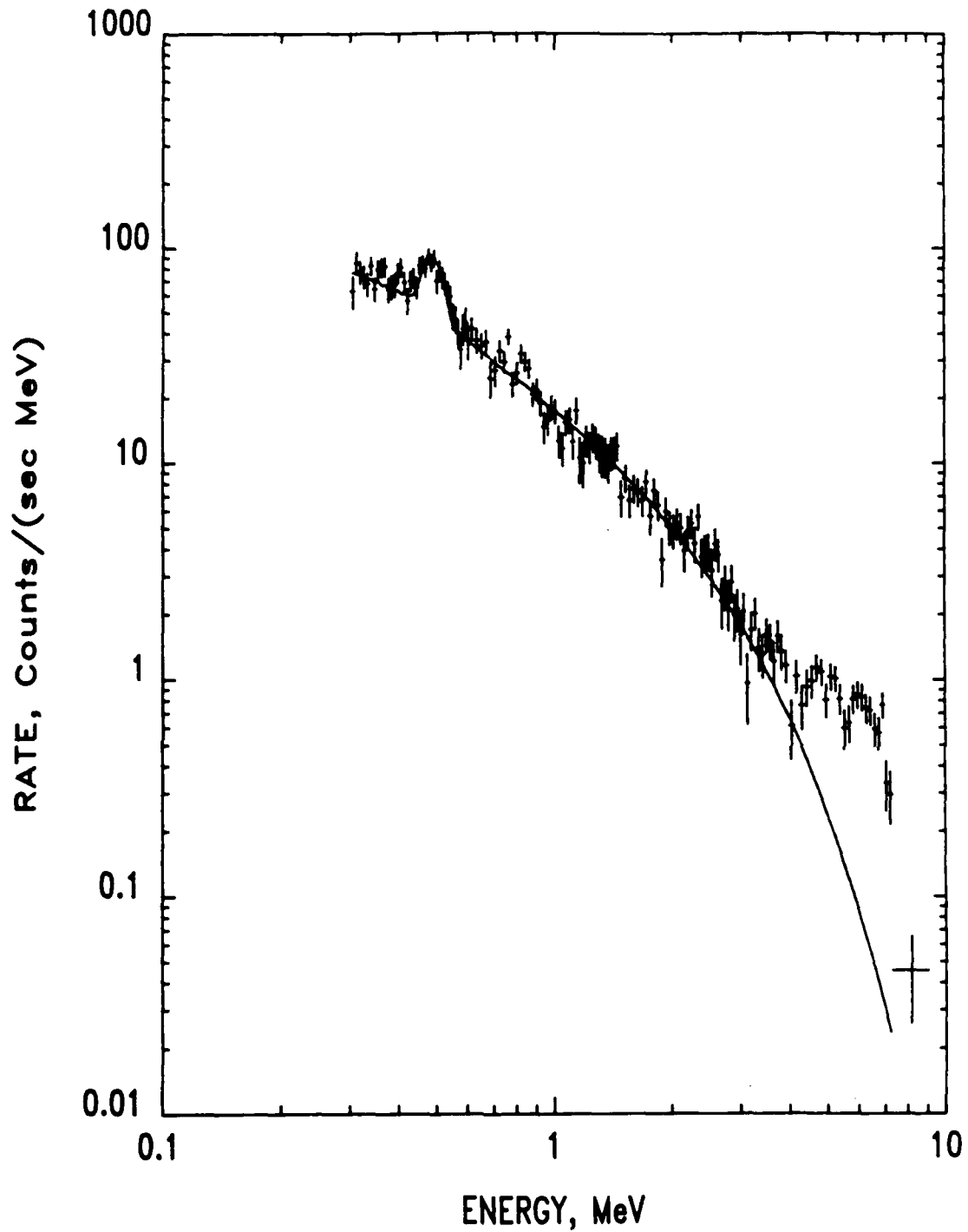


Fig. 6 — Integrated count-rate spectrum for close-approach sightings of the seven ROR-SATS in operation from 1980 to 1984. Total accumulation time is 1470 s. Curve shows composite of ^{235}U fission spectrum (under 50 g/cm^2) and narrow lines at 477 keV and 511 keV (under 7 g/cm^2) after being modified by the instrument response function.

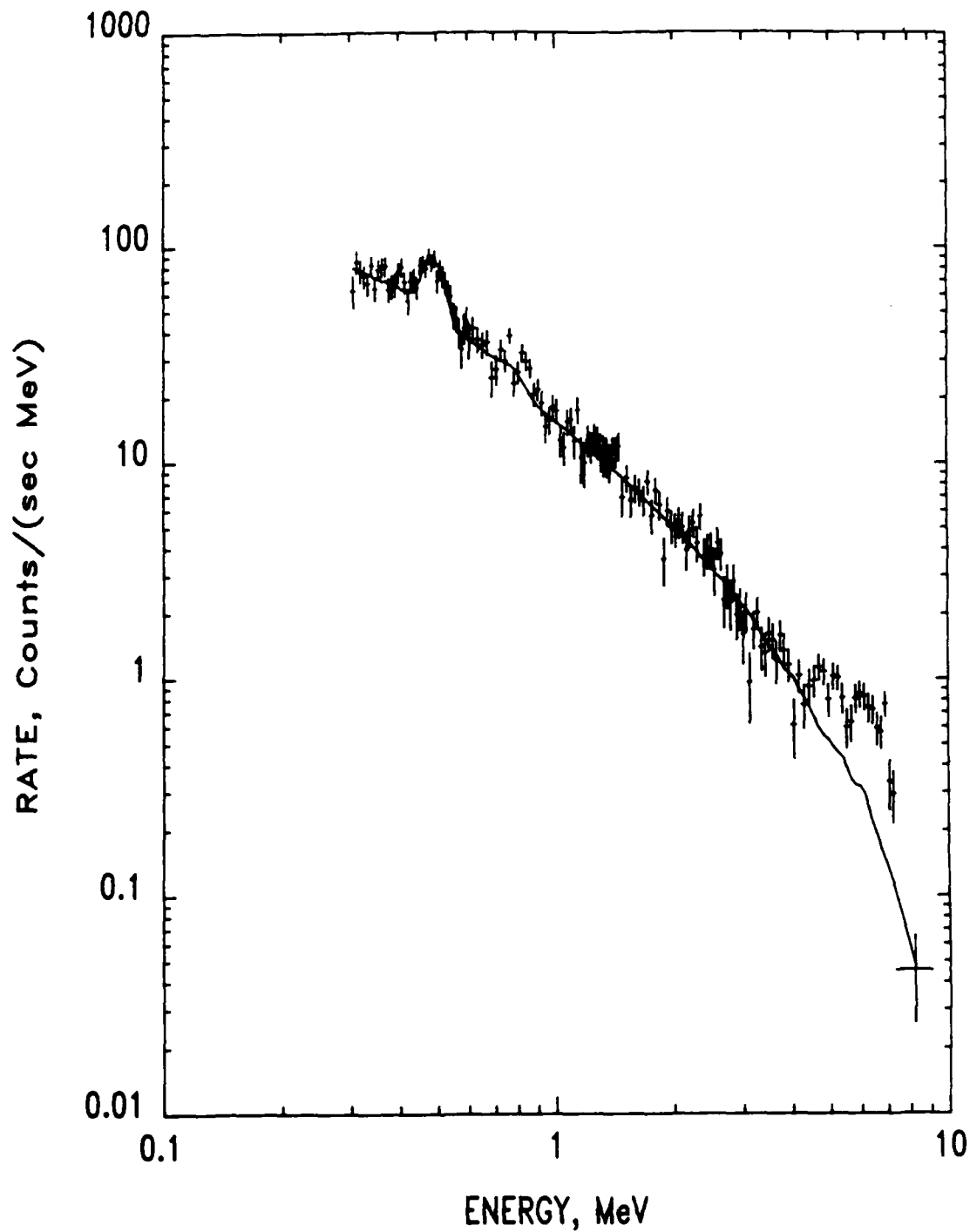


Fig. 7 — Integrated count-rate spectrum for close-approach sightings of the seven ROR-SATS in operation from 1980 to 1984. Total accumulation time is 1470 s. Curve shows composite of ^{235}U fission spectrum and spectrum from fast neutrons interacting in Mo (both components under 50 g/cm^2), and narrow lines at 477 keV and 511 keV (under 7 g/cm^2) after being modified by the instrument response function.

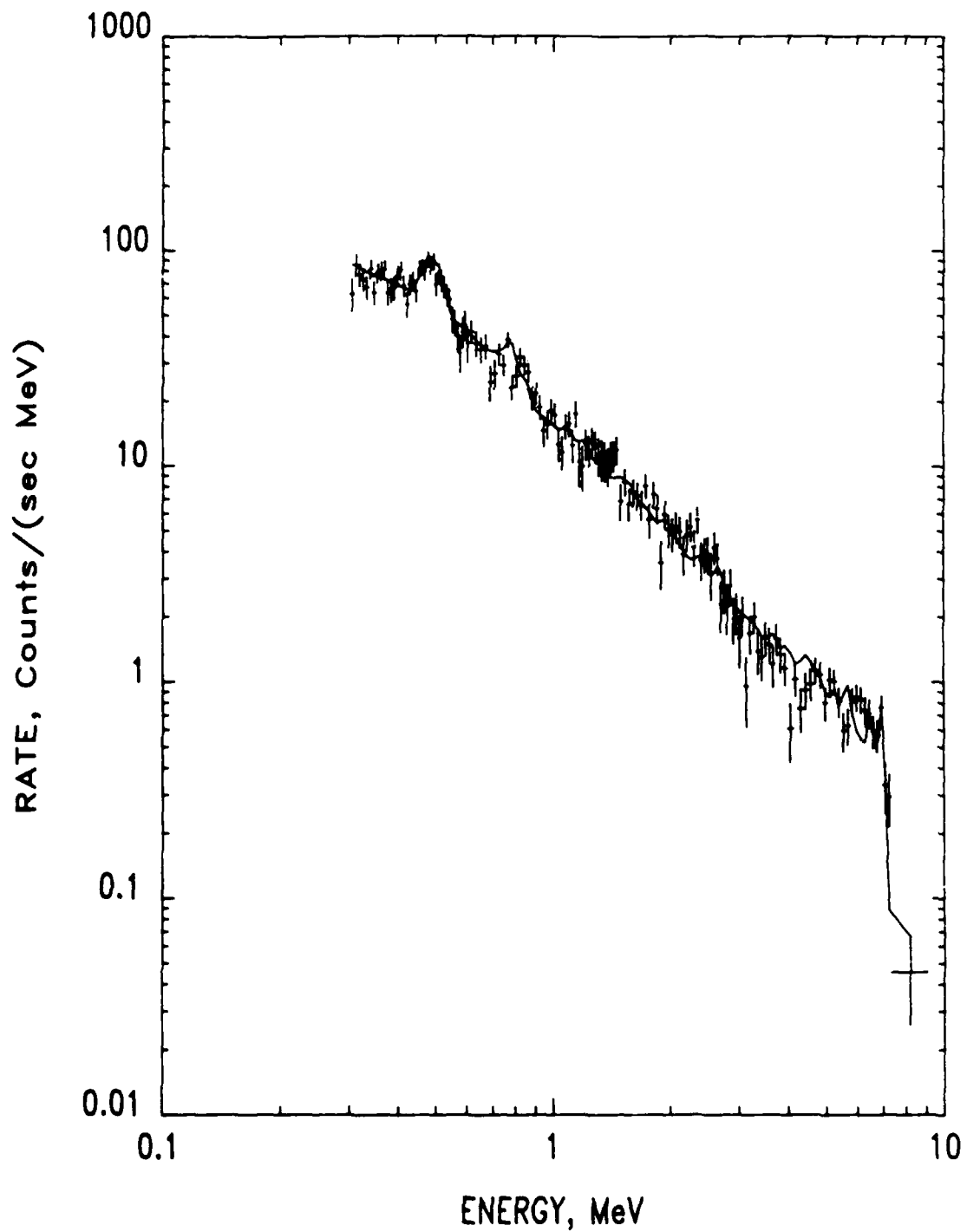


Fig. 8 - Integrated count-rate spectrum for close-approach sightings of the seven ROR-SATS in operation from 1980 to 1984. Total accumulation time is 1470 s. Curve shows composite of ^{235}U fission spectrum and Mo neutron capture spectrum (both under 50 g/cm^2), and narrow lines at 477 and 511 keV (under 7 g/cm^2), after being modified by the instrument response function.

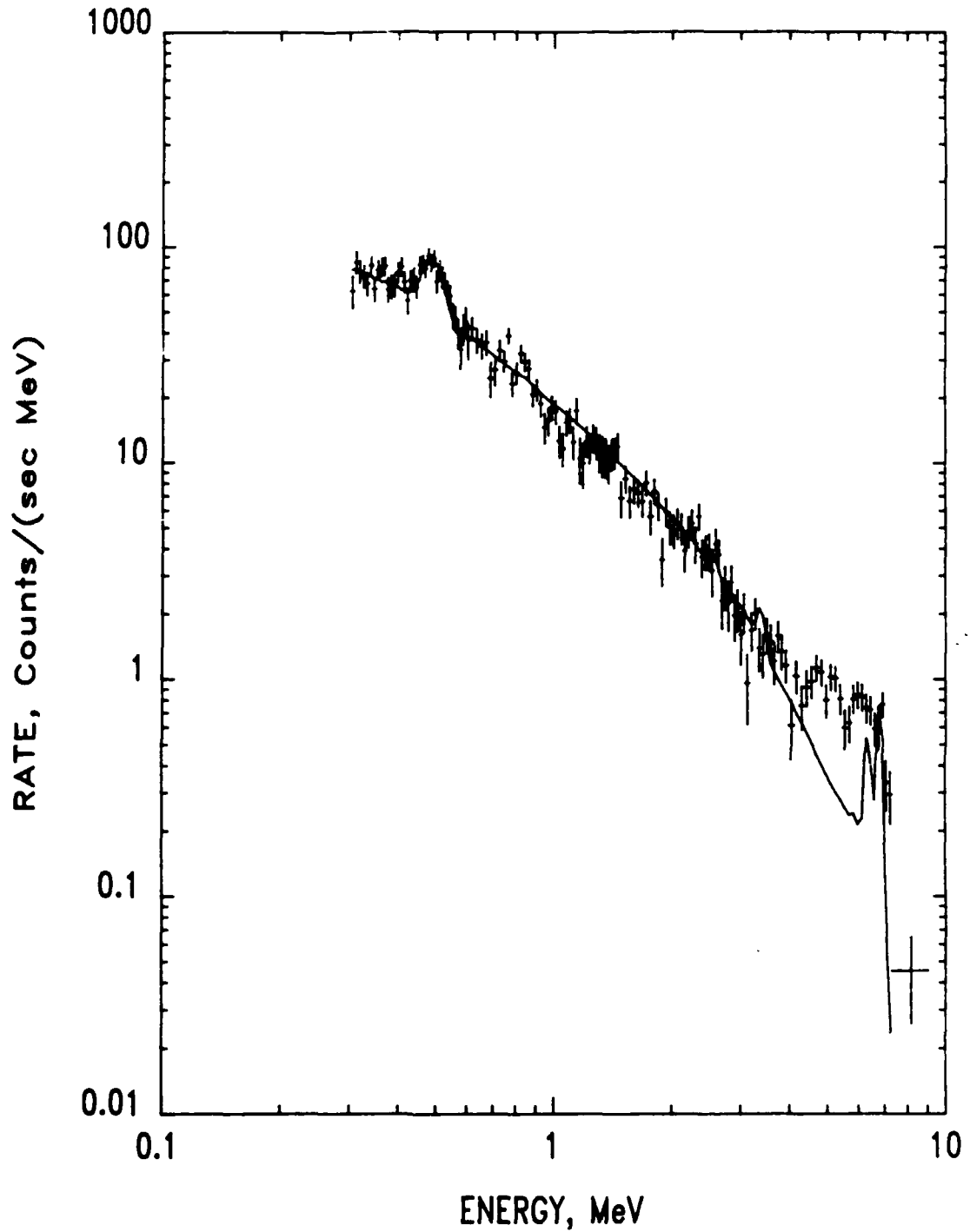


Fig. 9 — Integrated count-rate spectrum for close-approach sightings of the seven ROR-SATS in operation from 1980 to 1984. Total accumulation time is 1470 s. Curve shows composite of ^{235}U fission spectrum and Be neutron capture spectrum (both under 50 g/cm^2), and narrow lines at 477 and 511 keV (under 7 g/cm^2), after being modified by the instrument response function.

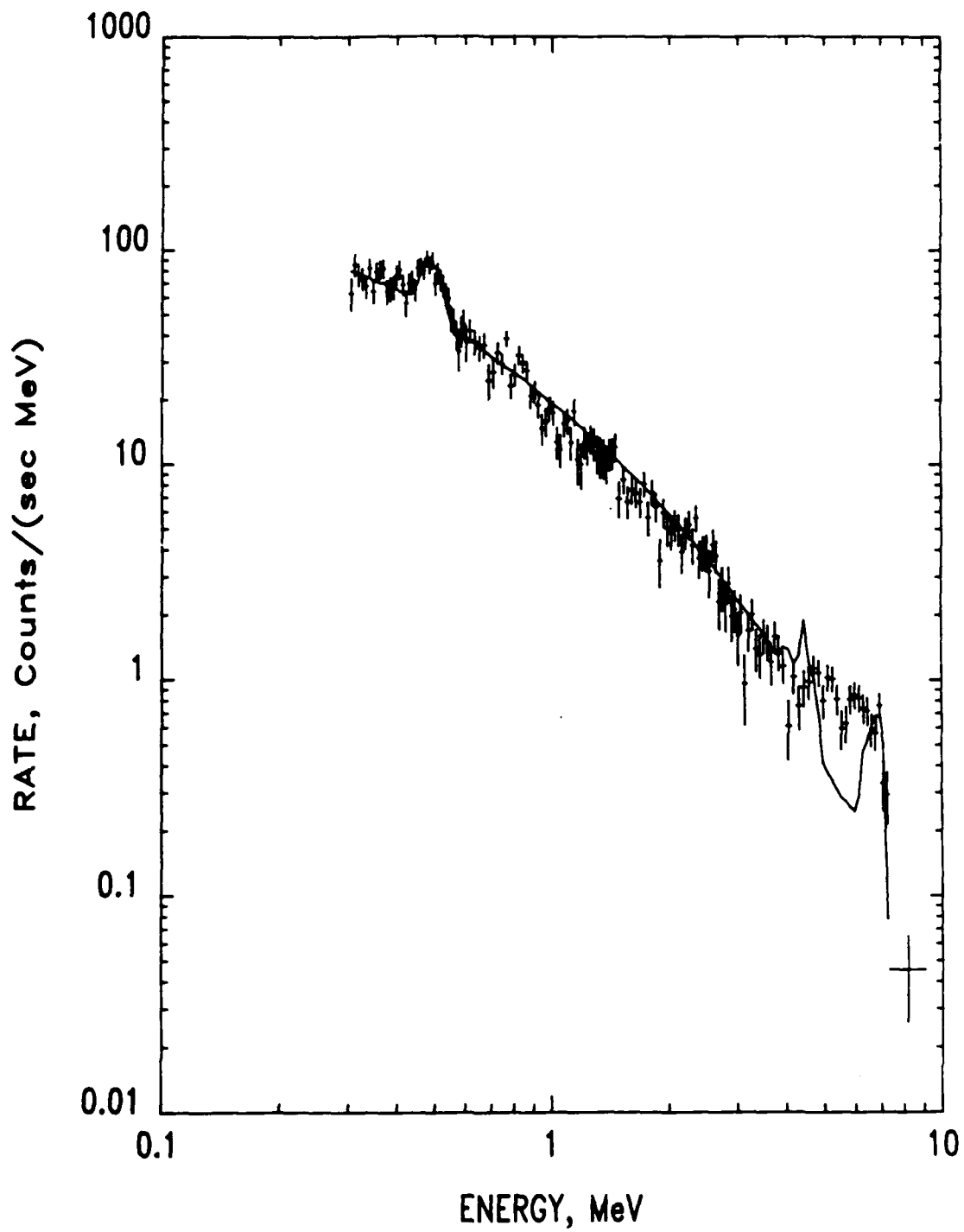


Fig. 10 - Integrated count-rate spectrum for close-approach sightings of the seven ROR-SATS in operation from 1980 to 1984. Total accumulation time is 1470 s. Curve shows composite of ^{235}U fission spectrum and B neutron capture spectrum (both under 50 g/cm^2), and narrow lines at 477 and 511 keV (under 7 g/cm^2), after being modified by the instrument response function.

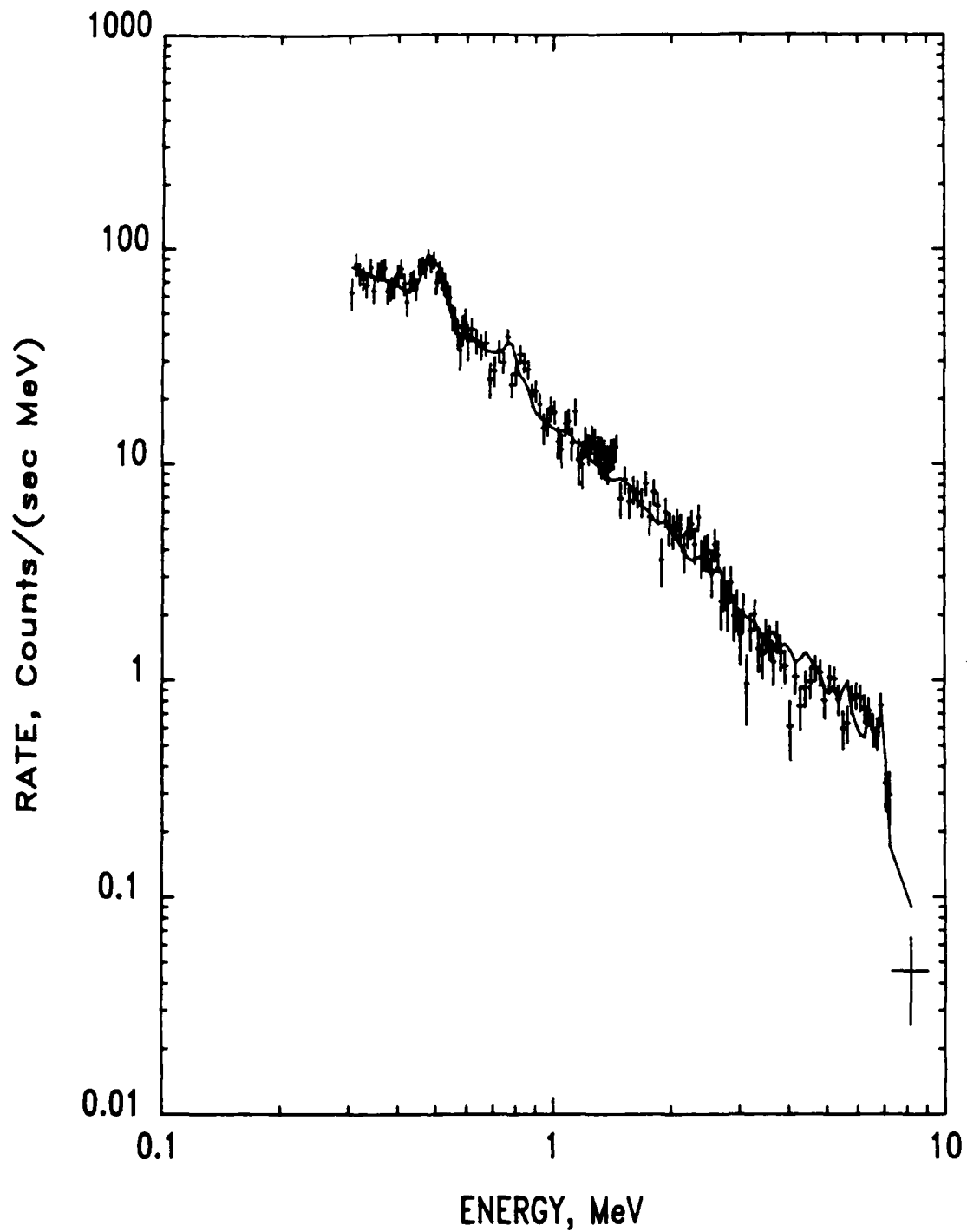


Fig. 11 — Integrated count-rate spectrum for close-approach sightings of the seven ROR-SATS in operation from 1980 to 1984. Total accumulation time is 1470 s. Curve shows composite of ^{235}U fission spectrum, Mo neutron capture spectrum (both under 50 g/cm^2), and narrow lines at 477 to 511 keV and Fe neutron capture spectrum (all under 7 g/cm^2), after being modified by the instrument response function.

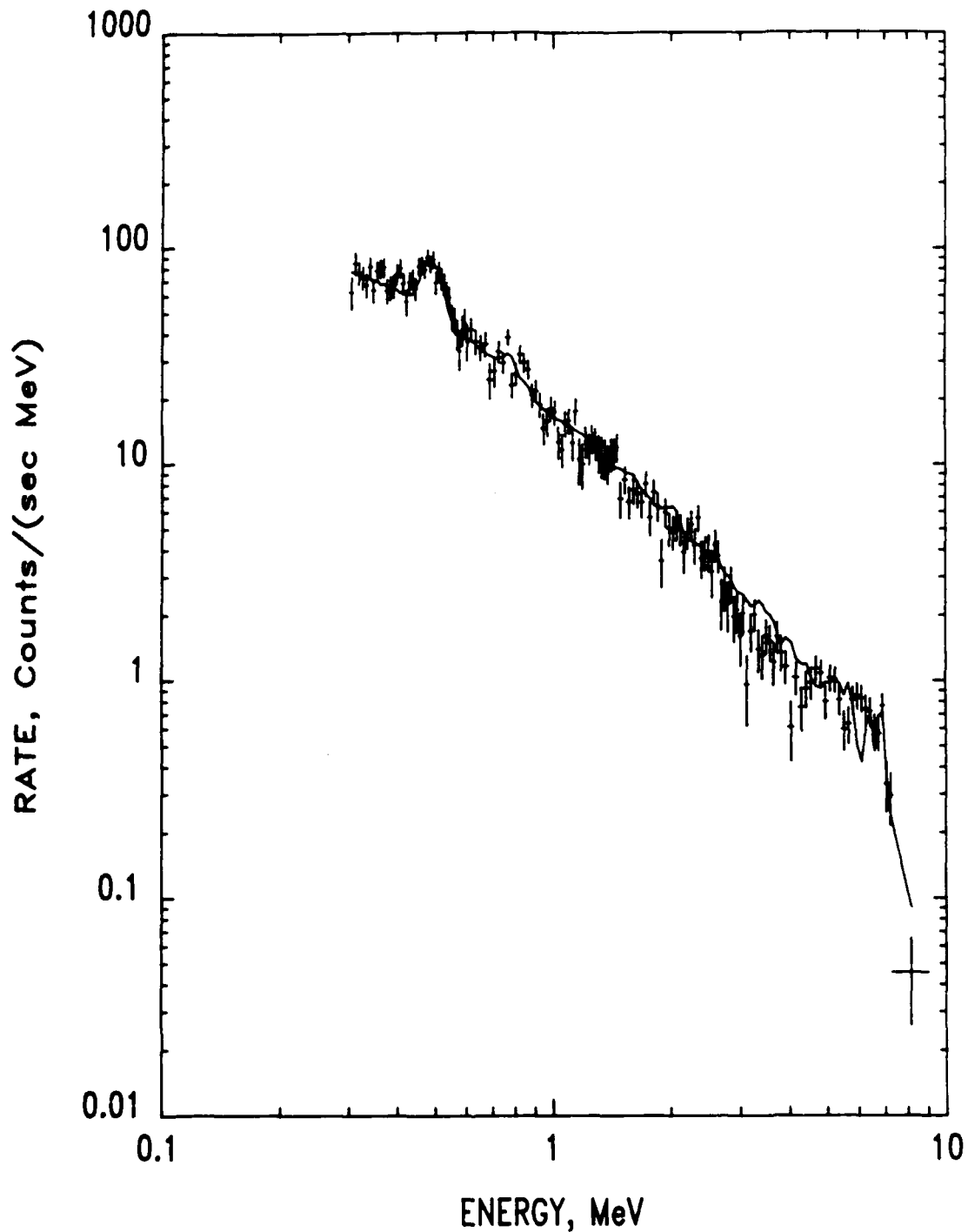


Fig. 12 — Integrated count-rate spectrum for close-approach sightings of the seven ROR-SATS in operation from 1980 to 1984. Total accumulation time is 1470 s. Curve shows composite of ^{235}U fission spectrum, and Mo, Na, K, Be neutron capture spectra (all under 50 g/cm^2), and narrow lines at 477 and 511 keV and Fe neutron capture spectrum (all under 7 g/cm^2), after being modified by the instrument response function.

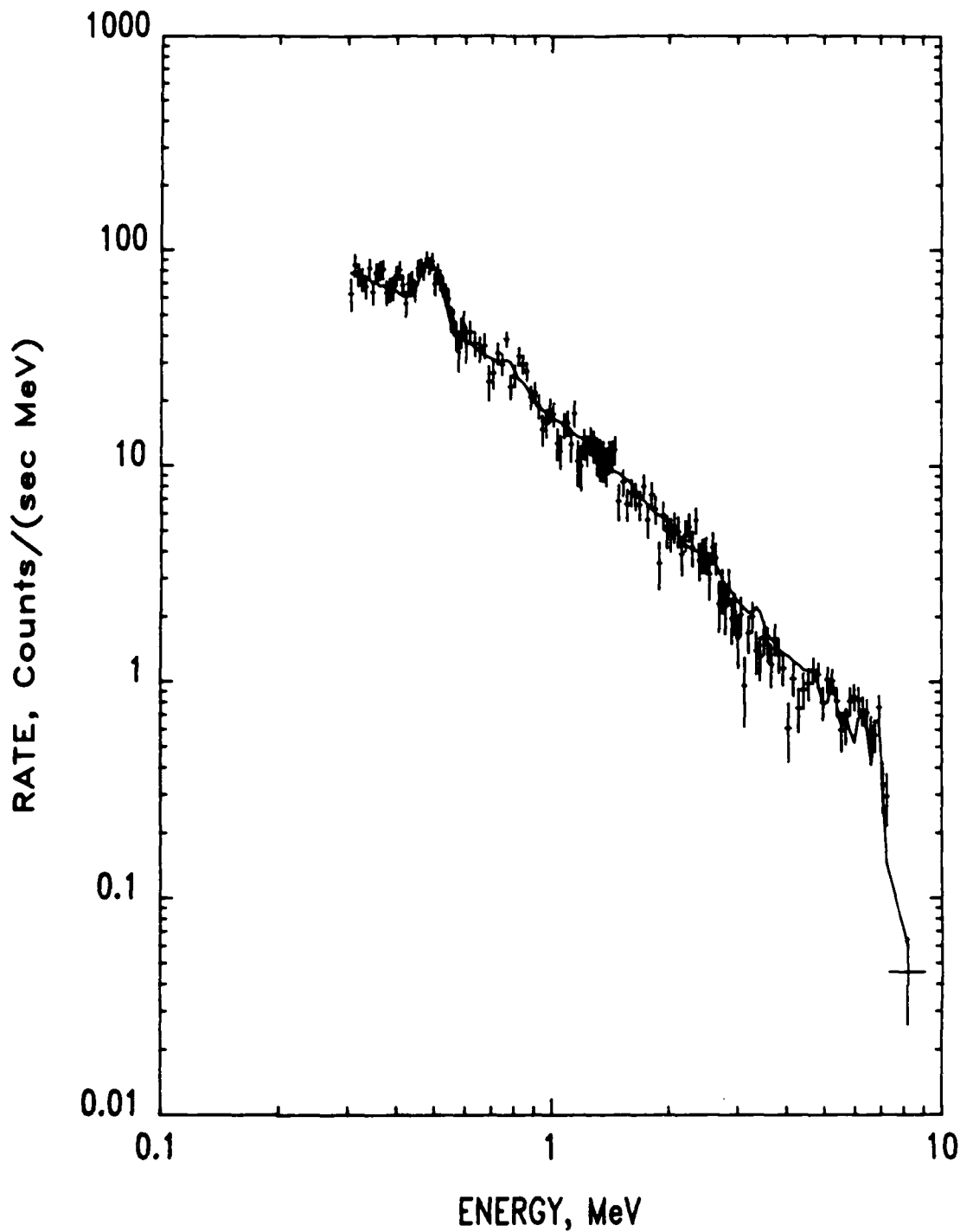


Fig. 13 — Integrated count-rate spectrum for close-approach sightings of the seven ROR-SATS in operation from 1980 to 1984. Total accumulation time is 1470 s. Curve shows composite of ^{235}U fission spectrum and Mo, Be, W neutron capture spectra (all under 7 g/cm^2), and narrow lines at 477 and 511 keV and Fe neutron capture spectrum (all under 7 g/cm^2), after being modified by the instrument response function.

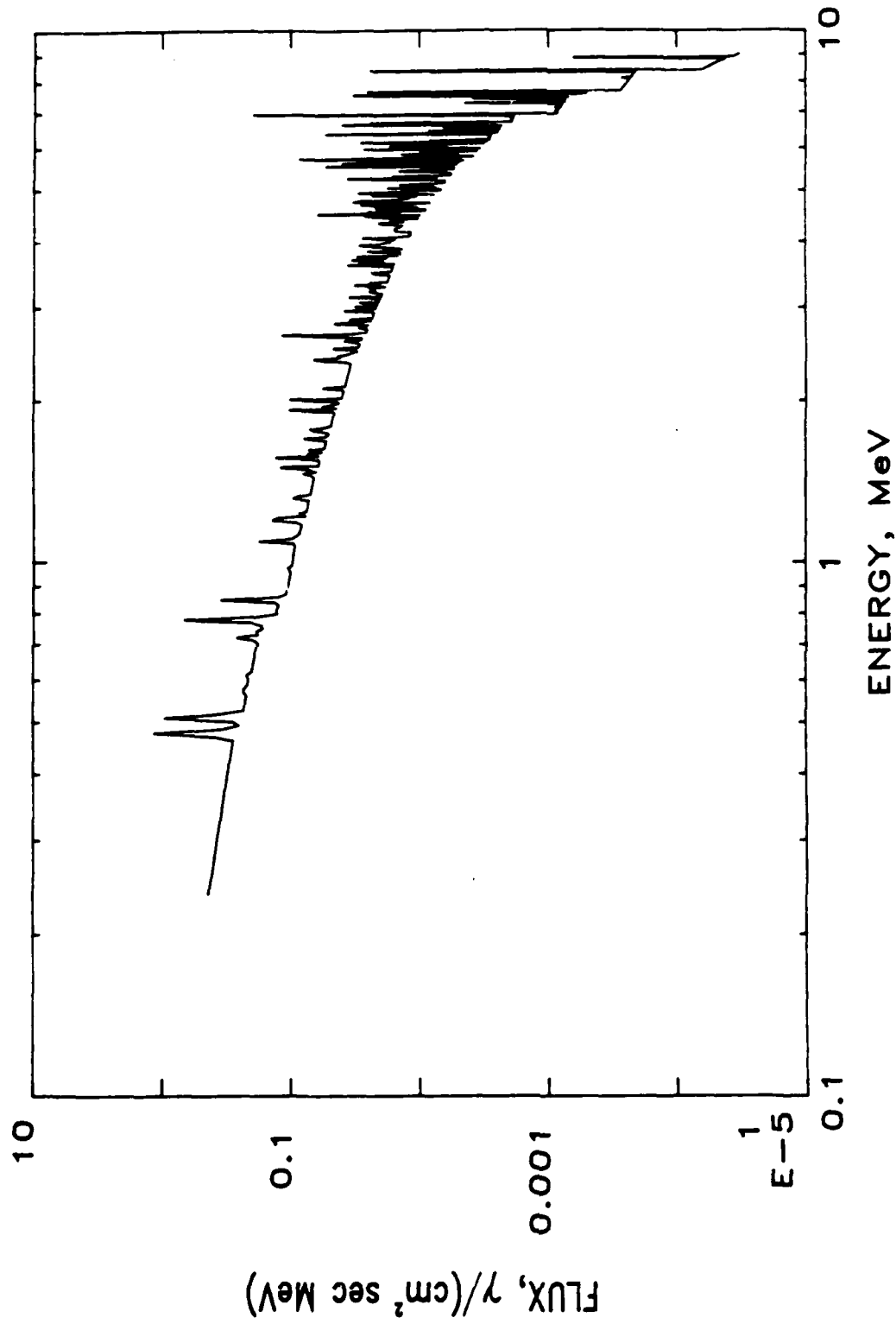


Fig. 14 — Estimate of the gamma-ray spectrum observed at a distance of ~ 300 km from a RORSAT. Spectrum includes ^{235}U fission and neutron capture on Mo (both under 50 g/cm^2), narrow lines at 477 and 511 keV (under 7 g/cm^2), and neutron capture on Fe (under 7 g/cm^2). The spectrum is plotted using the 476 channels of the SMM spectrometer; the spectrum using a germanium detector will exhibit even better resolution.